Development of Fire Hazard Index through Multispectral Indices and Geospatial Analysis

Afiqah Zahidah Anwarzaini., Nazirah Md Tarmizi*

Faculty of Built Environment, Universiti Teknologi MARA Cawangan Perlis, Arau Campus, Perlis, Malaysia

***Corresponding Author**

DOI: https://doi.org/10.47772/IJRISS.2026.10200608

Received: 04 March 2026; Accepted: 09 March 2026; Published: 23 March 2026

ABSTRACT

Wildfires are among the most destructive natural disasters due to their increased frequency, intensity, and duration. Countries in Southeast Asia (SEA), which primarily have tropical climates, have seen a few wildfire incidents in recent decades. To manage ecosystems and minimise disasters, effective surveillance systems are necessary. Thus, this paper aimed to derive a Fire Hazard Index (FHI) using multispectral indices through geospatial analysis, in parallel with the objectives of ascertaining the correlation coefficient using the Multiple Linear Regression (MLR) method and identifying the wildfire hazard zone in Perlis. Utilising high-resolution satellite imagery from Landsat 8, various significant spectral indices, including Land Surface Temperature (LST), Normalised Difference Vegetation Index (NDVI), Normalised Difference Moisture Index (NDMI), Normalised Difference Water Index (NDWI), Normalised Difference Drought Index (NDDI), and Normalised Burn Ratio (NBR), were combined and analysed. The correlation coefficients for the spectral indices used to develop the index were calculated using the Ordinary Least Squares (OLS) tool in ArcMap 10.5. The resultant coefficients were used to develop the FHI, and the wildfire hazard index for Perlis state was calculated using the Raster Calculator tool. The result indicates that the combined multispectral indices have a high predictive accuracy of 71% ($R^2 = 0.71$). The results of the hazard zone identification in Perlis, Malaysia, determined using our developed FHI model, reveal that the very high hazard zone was concentrated in the Kangar area during hot, dry weather. The resulting FHI map is an adaptable tool that local authorities may use to monitor long-term ecological recovery and establish wildfire mitigation strategies.

Keywords:- Fire Hazard Index, Hazard Assessment, Geospatial Analysis, Multispectral Indices, Remote Sensing

INTRODUCTION

Wildfires are emerging as one of the most disastrous natural disasters and have a substantial impact on the political stability, the resilience of human cultures and economies, and global ecosystems. Over the past few years, wildfires have increased in frequency, intensity, and duration worldwide. The main causes of these incidents include changes in land use, extended droughts, and the cumulative effects of climate change (Chew et al., 2022). In previous years, human activity was the primary source of wildfire incidents. However, since late 2019, conditions favourable to high-intensity wildfire behaviour have been fostered by high temperatures, powerful winds, and low relative humidity (Thangavel et al., 2023). The degraded areas prone to fire are mostly affected by dry conditions and the high temperatures imposed by climate change. Several indicators, including fuel moisture content, relative humidity, temperature, and precipitation, are used to measure wildfires, including unintentional forest fires and bush fires (Bandara, Navaratnam and Rajeev, 2023). Globally, this calamitous phenomenon has evolved into an annual occurrence.

In recent decades, Southeast Asian (SEA) countries, characterised by tropical climates, have experienced numerous wildfires. In Thailand, protected forest regions experienced 4,207, 4,982, and 6,685 wildfires during the dry seasons in 2014, 2015, and 2016, respectively (Burapol & Nagasawa, 2016). In addition, forest fires in

Brunei Darussalam increased by 80%, particularly between 2007 and 2016 (Zahran, Shams & Said, 2020). In Indonesia, wildfires damaged approximately 135,000 hectares of forested areas, with the South Sumatra region experiencing the highest number of reported incidents in 2019 (Rendana, 2023). Also, Vietnam had 4,571 forest fires from 2009 to 2018, which destroyed almost 22,000 acres of forest, and the worst year was 2010, when 6,723 hectares were burned (Nguyen & Tong, 2023).

In a similar vein, Malaysia frequently experiences devastating wildfires in its forested areas, particularly during the dry season. According to data, Malaysia recorded 1,232 forest fire events between 1992 and 1998 (Jamaruppin et al., 2016). Sabah experienced forest fire incidents affecting an area of about 1 million hectares in 2015 (Fisal, Lintangah & Ismenyah, 2017). Additionally, Johor experienced a forest fire in August 2019 that spread over 2.4 hectares (Chew et al., 2022). A temporal analysis conducted by Anwarzaini & Tarmizi (2025) shows a significant increase in fire occurrences in Perlis, Malaysia, with 63.11% of wildfire occurrences recorded from 2014 to 2024 involving shrubs and forest fires. In other findings, forest fires in Peninsular Malaysia have resulted in substantial losses, including the devastation of local flora and fauna, across approximately 12,000 hectares of peat forest (Mat Deli, 2023). Although most fires in Peninsular Malaysia were small-scale, involving fewer than 100 hectares, the rise in frequency and intensity driven by hot, dry weather remains concerning (Chew et al., 2023). The increasing frequency and intensity of wildfires in recent years have raised significant concerns about their ecological and societal impacts, requiring timely and accurate responses to mitigate damage (Tarmizi, Anwarzaini & Fisol, 2025). Consequently, it is imperative to implement frequent and rapid monitoring of high-risk areas.

In the past, watch towers and optical cameras installed in specific locations were used to monitor this data. Despite their accuracy, these methods require significant effort, are difficult to implement in rugged terrain, and lack the spatial continuity essential for regional or national monitoring. Traditional monitoring techniques are useless as wildfires become more dangerous and unpredictable. Post-fire environments are known to be very challenging to assess because their physical landscape undergoes dramatic changes that can lead to severe ecological degradation and increased susceptibility to erosion and flooding (Tarmizi, Anwarzaini & Fisol, 2025). Thus, a comprehensive environmental monitoring program is feasible through the integration of Geographical Information Systems (GIS) and Remote Sensing (RS), as these technologies can be used to track natural disasters and assess their environmental impacts (Tarmizi & Rizwan, 2024). Furthermore, satellite images can be utilised to derive numerous spectral indices that are valuable for various applications, including wildfire monitoring (Thangavel et al., 2023), and they can cover larger monitoring areas and extremely remote areas. This methodology will be implemented to generate the fire hazard index and forecast wildfire hazard zones.

Spectral indices in Remote Sensing have been employed in most Malaysian studies to monitor wildfire occurrence; however, most of these studies have focused on evaluating the severity of burning after a fire. There are significant gaps in research on generating wildfire hazard indexes and estimating wildfire hazard zones using multispectral indices. Therefore, this study aimed to utilise Geospatial analysis to derive a Fire Hazard Index (FHI) that is suitable for tropical climate regions using LST, NDVI, NDMI, NDWI, NDDI, and NBR. The following objectives were prioritised: to ascertain the correlation coefficient through the Multiple Linear Regression method and to identify the wildfire hazard zone in Perlis. Nevertheless, this investigation examines only the environmental conditions in Perlis state during the dry season, which typically occurs in March, and does not consider the other months of that year.

METHOD

This study employed GIS software and remote sensing data to derive a Fire Hazard Index (FHI) for tropical regions and identify wildfire hazard zones. The process comprises the determination of the study area, the acquisition and preprocessing of data, the derivation of each index, the determination of coefficients using MLR, the development of FHI, and the identification of the wildfire hazard zone. The Landsat 8 OLI/TIRS image obtained in March 2024 and statistical information on fire incidents in forests, bushlands, and agricultural areas were the datasets utilised in this study. According to The Global Historical Weather and Climate Data, Perlis experienced the warmest weather in March with an average of 33°C. This study specifically examine and estimate the wildfire hazard during the peak of the hot and dry season, thus underlining the utilization of the satellite images obtained in March. In addition, the Landsat 8 OLI/TIRS was chosen due to its higher temporal

and spatial resolution that suit the size of the study area. The data will be processed in ArcMap 10.5 using the Spatial Analysis toolbox, which comprises the Raster Calculator tool, the Extract Multi Value tool, the Ordinary Least Squares (OLS) tool, and the Kernel Density Estimation (KDE) tool. The Raster Calculator tool was used to calculate the index value because it allow mathematical flexibility and to ensure the output are as precise as the input data. The results will be presented as an index equation and a hazard map. Figure 1 illustrates the general workflow of this study.

Study Area

The study was carried out in Perlis, Malaysia, which is located between latitudes 6°30' N and longitudes 100°15' E. The major landscape consists of semi-deciduous forest, grasslands, and agricultural fields. Three political jurisdictions, which are Padang Besar, Kangar, and Arau, were used to define the study area. Despite being the smallest state in Malaysia, Perlis frequently experiences higher temperatures than other states, with a maximum recorded temperature of 40°C, particularly during the southwest monsoon, which is usually hotter and drier. The state recorded an average temperature 0.17% higher than Malaysia's, and the warmest and driest months were February and March. Figure 2 demonstrates the map of the studied area.

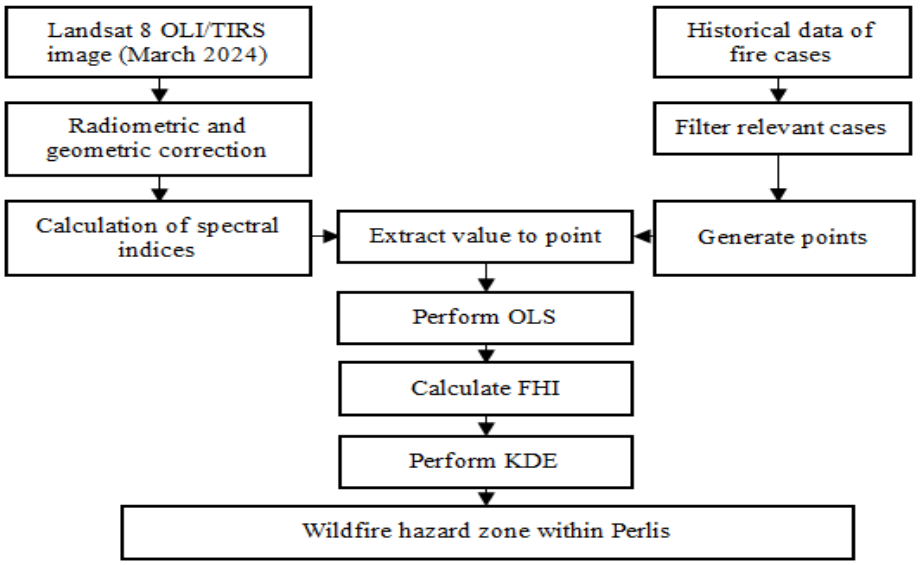

Figure 1 The general workflow of the proposed study

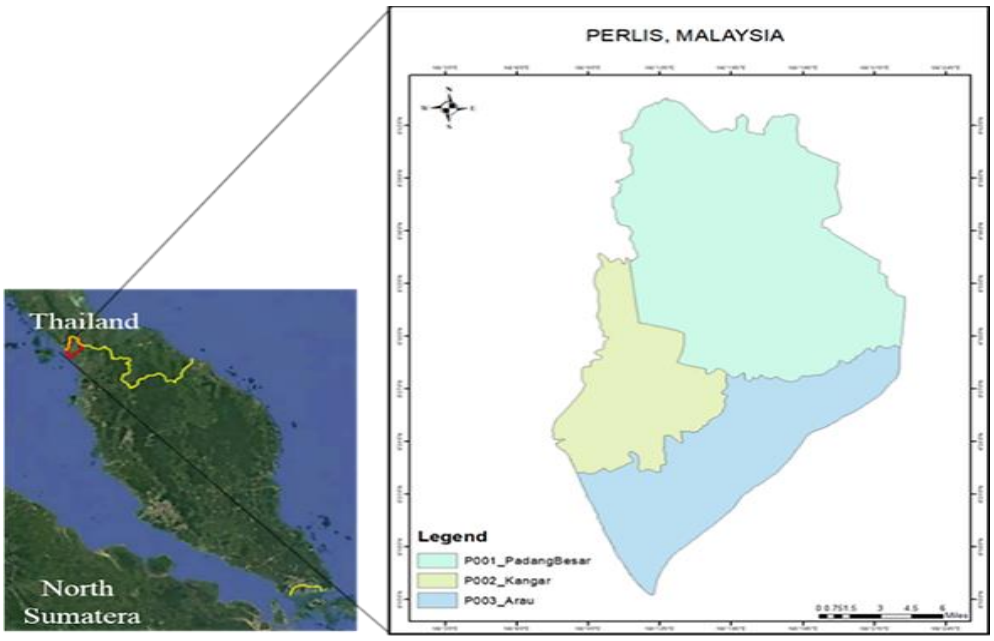

Figure 2 Map of the studied area

Data Acquisition and Preprocessing

The USGS Earth Explorer, an open-source database, provided the Landsat 8 OLI/TIRS image. The spectral bands that were selected, specifically bands 3, 4, 5, 6, 7, and 10, were downloaded in Geo-TIFF format. The satellite image was carefully selected in March 2024, with cloud cover less than 20%. The images were preprocessed in ArcMap 10.5 to correct radiometric and geometric errors. To eliminate haze, cloud cover and adjust the sun angle parameter, a radiometric correction was performed using the Raster Calculator tool. The Quality Assessment Bands tool was then used to preprocess the image to ensure the quality of each selected band. The administrative boundary of Malaysia was retrieved in SHP format from the Humanitarian Data Exchange website. Perlis state's boundary and political zones were clipped with the Clip tool and labelled as P001 (Padang Besar), P002 (Kangar), and P003 (Arau), respectively. The Raster Clip tool is also used to trim the rectified raster data to reduce processing time. To ensure proper data overlap, the datasets were projected into the WGS84 global coordinate system using the Projection and Transformation tool. To supplement the analysis, historical data on wildfire incidents in Perlis from 2014 to 2024 were obtained from the Perlis State Fire and Rescue Department. After filtering the statistical data, fire cases of bushlands, agricultural fields, and forests were extracted.

The Derivation of the Multispectral Indices

The Raster Calculator utility in ArcMap 10.5 was used to derive spectral indices from the corrected bands of the Landsat 8 OLI/TIRS image. According to (Moisa et al., 2023), the Land Surface Temperature (LST) was obtained through a mono-window method, which included the conversion of digital numbers to radiance, the transformation of radiance to brightness temperature, the assessment of vegetation proportion via NDVI, the calculation of land surface emissivity, and the derivation of LST. Table 1 outlines the formulas necessary for the derivation of LST, whereas Table 2 describes the formulas employed to generate NDVI, NDMI, NDWI, NDDI, and NBR as proposed by (Rendana, 2023), (Nguyen & Tong, 2023), (Moisa et al., 2023), and (Anucharan, 2025).

Table 1. The formulas used to derive LST using the mono-window method

Steps	Formulation used	Description
i.	The conversion of a digital number to radiance $L_\lambda = M_L \times Q_{cal} + A_L$	L_λ is the top-of-the-atmosphere radiance. M_L is the band 10 radiance multiplicative constant Q_{cal} is the corresponding band 10 A_L is the band 10 radiance additive constant
ii.	The conversion of radiance to brightness temperature $BT = \frac{K2}{\ln\left(\frac{K1}{L_\lambda} + 1\right)}$	BT is the brightness temperature in Kelvin $K2$ is the K2 band 10 thermal conversion constant $K1$ is the K1 band 10 thermal conversion constant L_λ is the top-of-the-atmosphere radiance
iii.	The determination of vegetation proportion using NDVI $P_v = \left(\frac{NDVI - NDVI_{min}}{NDVI_{max} - NDVI_{min}}\right)^2$	P_v is the vegetation proportion $NDVI$ is the corresponding NDVI raster $NDVI_{min}$ is the minimum value of the NDVI $NDVI_{max}$ is the maximum value of the NDVI
iv.	The determination of land surface	ε is the land surface emissivity

	emissivity $\varepsilon = 0.004 \times P_v + 0.986$	P_v is the vegetation proportion
v.	The determination of LST using brightness temperature and corrected emissivity $LST = \left[\frac{BT}{1 + (W \times BT/P)\ln\varepsilon}\right] - 273.15$	LST is the land surface temperature in Celsius BT is the brightness temperature W is the wavelength of the emitted radiance constant P is the constant value which is equal to 1.438×10−2 m K ε is the land surface emissivity

Table 2. The formulas used to derive NDVI, NDMI, NDWI, NDDI, and NBR

No.	Formulation used	Description
i.	$NDVI = \frac{\rho_{NIR} - \rho_R}{\rho_{NIR} + \rho_R}$	$NDVI$ is the normalised difference vegetation index ρ_{NIR} is the near infrared band, which corresponds to band 5 ρ_R is the red band, which corresponds to band 4
ii.	$NDMI = \frac{\rho_{NIR} - \rho_{SWIR}}{\rho_{NIR} + \rho_{SWIR}}$	$NDMI$ is the normalised difference moisture index ρ_{NIR} is the near infrared band, which corresponds to band 5 ρ_{SWIR} is the short-wave infrared band, which corresponds to band 6
iii.	$NDWI = \frac{\rho_{GREEN} - \rho_{NIR}}{\rho_{GREEN} + \rho_{NIR}}$	$NDWI$ is the normalised difference water index ρ_{GREEN} is the green band, which corresponds to band 3 ρ_{NIR} is the near infrared band, which corresponds to band 5
iv.	$NDDI = \frac{NDVI - NDWI}{NDVI + NDWI}$	$NDDI$ is the normalised difference drought index $NDVI$ is the normalised difference vegetation index $NDWI$ is the normalised difference water index
v.	$NBR = \frac{\rho_{NIR} - \rho_{SWIR2}}{\rho_{NIR} + \rho_{SWIR2}}$	NBR is the normalised burned ratio ρ_{NIR} is the near infrared band, which corresponds to band 5 ρ_{SWIR2} corresponds to band 7

The Correlation Analysis Using MLR

The statistical analysis procedure that employed MLR was conducted by extracting spectral index values and combining them into a single feature layer. Prior to data extraction, the fire case data was loaded into the software, and point features were generated. The Integrate tool was employed to cluster the point data with a tolerance of 500 meters. The reason for this procedure is that fire cases within a 500-meter radius were presumed to represent the same location. The Collect Event tool was utilised to amalgamate the integrated point data into weighted point data, reflecting the frequency of occurrences at each location. Subsequently, the Extract Multi Values to Points tool was used to extract the calculated spectral index values, which were then combined with the weighted point data. The retrieved values can be evaluated in the attribute table of the point feature layer. The computation of correlation coefficients was executed utilising the Ordinary Least Squares (OLS) method. The fire incidents were designated as the dependent variable, while the spectral indices were the independent variables. The report was produced, and the correlation coefficients for each spectral index were acquired.

The Development of WHI and Identification of Wildfire Hazard Zone

The Fire Hazard Index (FHI) for Perlis state was developed by utilising the intercept constant and the calculated correlation coefficients of the spectral indices. The derived index was calculated using the Raster Calculator tool, resulting in a new raster layer. The resultant FHI value was interpolated using the Kernel Density Estimation (KDE) tool to pinpoint regions with elevated index values. The fire case points were designated as an input feature, while the WHI value was identified as the population field. The program will interpolate the WHI value and pinpoint wildfire hotspots. The output features were categorised into five classes: "Very High Hazard," "High Hazard," "Moderate Hazard," "Low Hazard," and "Very Low Hazard," yielding a hazard zone map.

RESULTS AND DISCUSSION

Results

The rise in wildfire frequency necessitates an approach for monitoring and identifying incident hotspots. This framework helps local authorities mitigate hazardous activities, such as burning crop residue or operating heavy machinery in potentially hazardous zones, particularly during the hot, arid season. Table 3 presents the correlation between multispectral indices and wildfire occurrence in Perlis, derived from OLS processing. The table indicates that the FHI model was statistically significant, accounting for 71% of the variance in the data (R2 = 0.71). The selected spectral indices are well-suited to the model, as evidenced by the high R^2 value.

Table 3. Result of the correlation model between multispectral indices and wildfire occurrence

Variable	R^2	Standard error	p-value
FHI	0.717	1.094	0.0001

Figure 3 shows the correlation coefficients for each spectral index. The graphic shows that NDMI and NDWI exhibited a negative correlation, whereas the other indices showed a positive correlation with wildfire occurrence. The highest coefficient was observed in NBR, followed by NDDI, with values of approximately 20 and 15, respectively, suggesting that these indices are the most influential factors. Conversely, LST exhibits the lowest coefficient, followed by NDMI, which approaches 0, indicating that these indices are the least significant influential factors in the model. The derived FHI equation from the computed coefficients is presented in Equation 1.

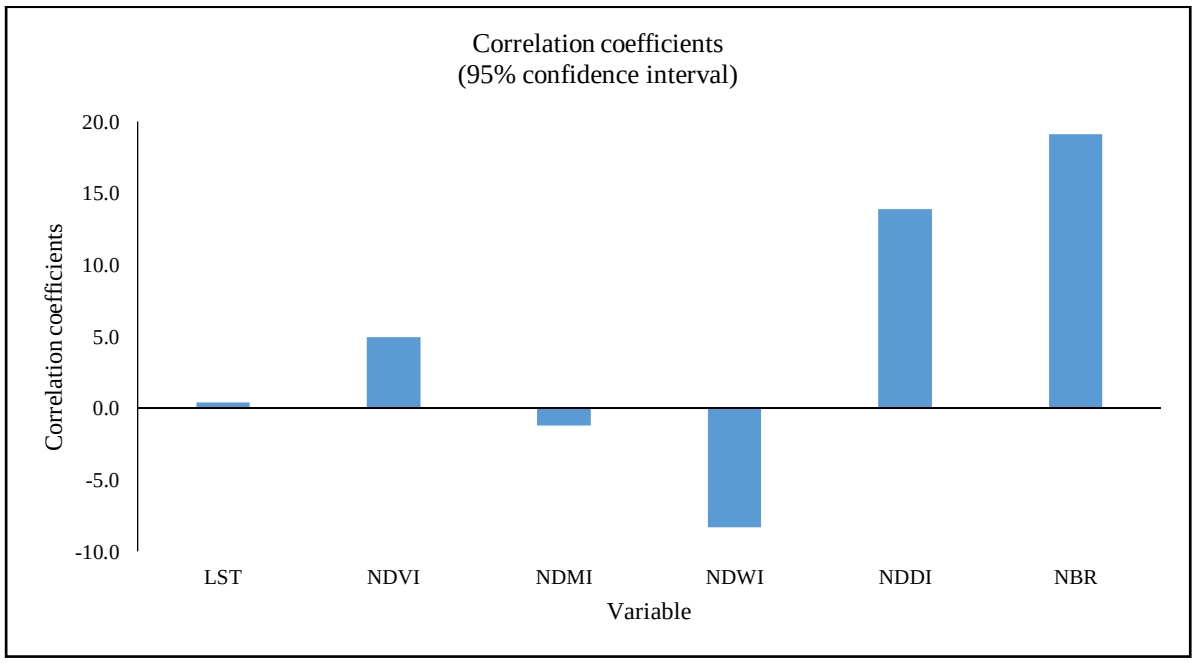

Figure 3 The standardised coefficients of the chosen spectral indices

Equation 1. The FHI equation to identify the wildfire hazard zone in Perlis

$$WHI=-9.460+0.366x_1+4.946x_2-8.330x_3-1.218x_4+13.876x_5+19.112x_6$$

Where x_1 is LST, x_2 is NDVI, x_3 is NDWI, x_4 is NDMI, x_5 is NDDI, and x_6 is NBR. The derived FHI equation from the computed coefficients is presented in Equation 1. The wildfire hazard zone in Perlis state was determined by applying the derived index using the Raster Calculator tool, as illustrated in Figure 4. Five zones were classified based on the results: "Very High Hazard", "High Hazard", "Moderate Hazard", "Low Hazard", and "Very Low Hazard". According to the figure, during the hot and dry season, the "Very High Hazard" zone was predominantly located in the Kangar area, coinciding with the recorded 29 fire incidents in March 2024. The Padang Besar area had two "Very High Hazard" zones, specifically at the main town of Padang Besar, Titi Tinggi, and Chuping, coinciding with the reported cases of 15, 13, and 7 incidents during the studied period, respectively. The region predominantly consisted of developed areas and grasslands, which were especially susceptible to ignition due to the sparse canopy and elevated radiation from built structures. A few locations in the Arau area were classified as "High Hazard" zones, which coincide with the area's low number of reported cases. In contrast, the "Very Low Hazard" was identified in the forested region of Nakawan Range, which includes Perlis State Park and Bukit Ayer Eco Forest Park. The region predominantly consisted of dense forest, which is less susceptible to ignition during the hot, arid season owing to its elevated canopy density and substantial water retention capacity. Figure 5 demonstrate the ground data captured after a wildfire outbreak in February 2026, commencing the beginning of the hot an dry season in Perlis. The location of the wildfire occurrence was in accordance to the interpolation of the hazard zone and past wildfire events. The historical events of wildfire over a decade was demonstrated in Figure 6.

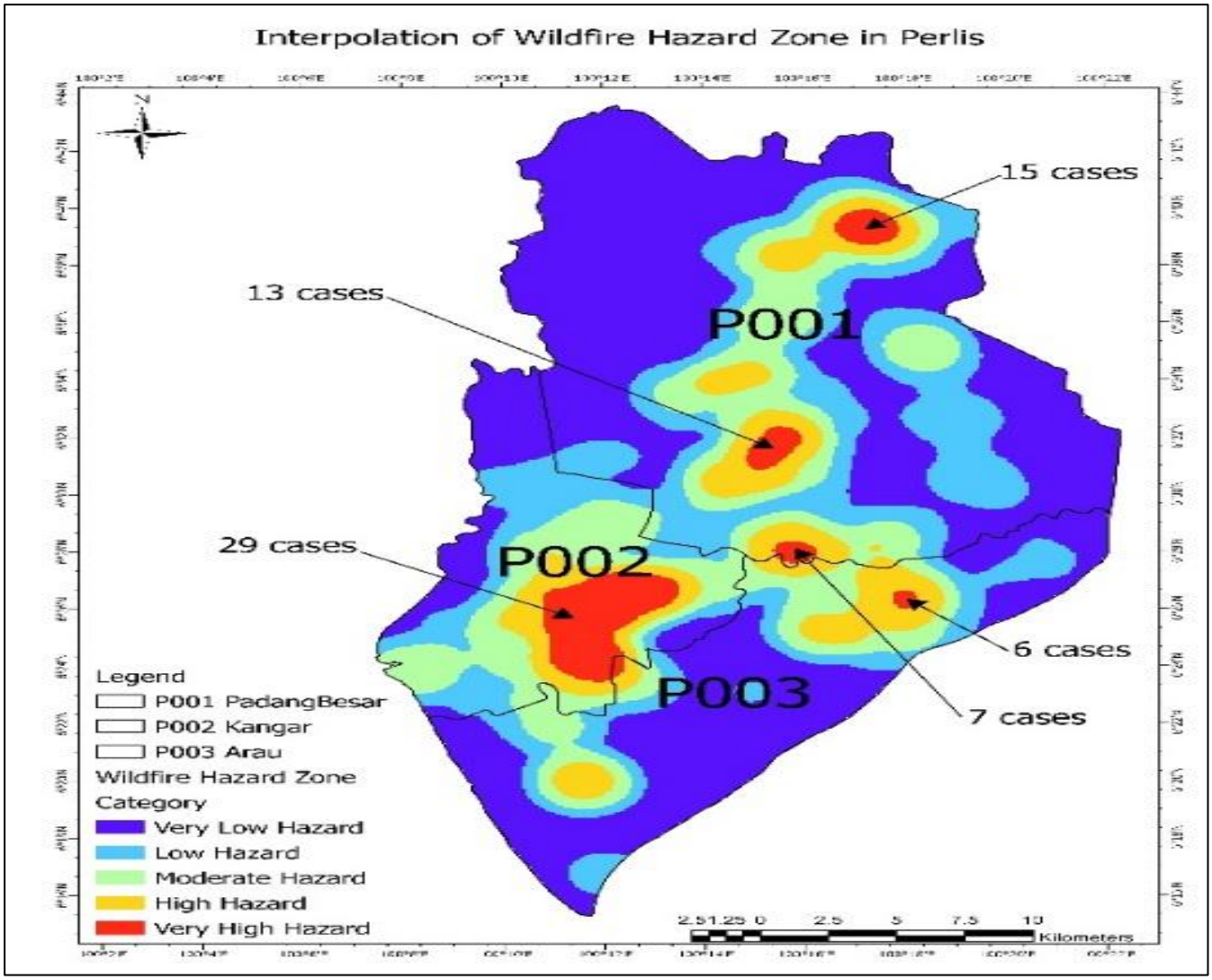

Figure 4 The projected wildfire hazard zone and past fire cases within Perlis state

Figure 5 The ground truth data taken on February 2025 near Bukit Lagi, Kangar, Perlis

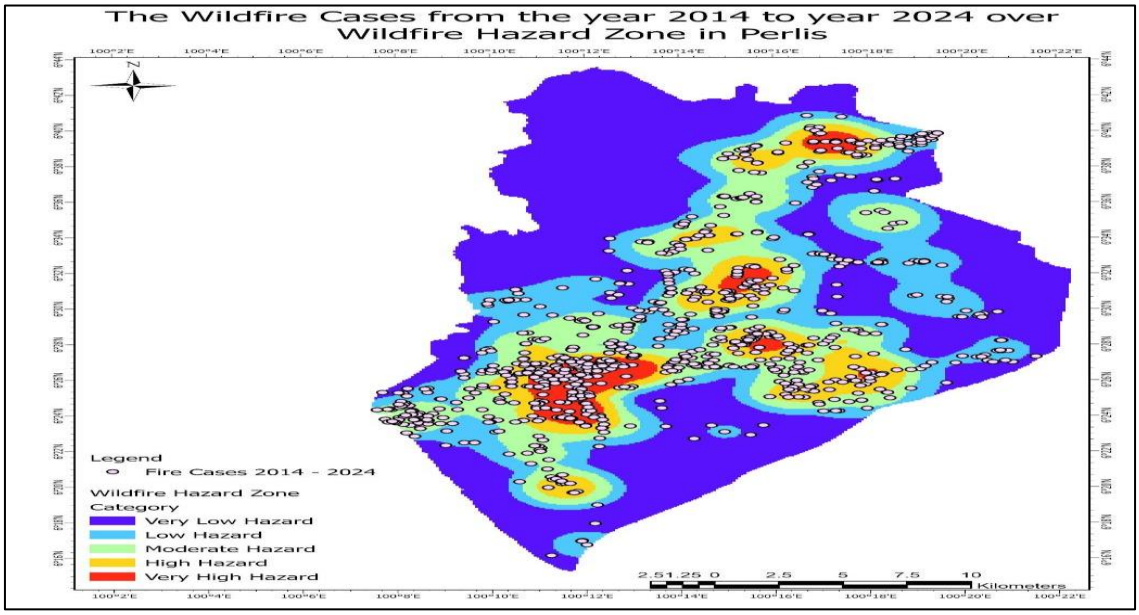

Figure 6 The overlay of projected wildfire hazard zone with past fire occurrence from the year 2014 to year 2024 in Perlis

DISCUSSION

The results of this study show that multispectral indices derived from satellite data are highly useful predictors of fire danger, as they reflect moisture levels, vegetation health, and surface temperatures. The NBR and NDDI are the most influential factors, as illustrated by the correlation coefficients for the spectral indices shown in Figure 3. Conversely, the LST was the least significant variable in the model. This result implies that during the extended hot, dry weather, LST reached its absolute limit. It can be inferred that the vegetation was severely dehydrated, as this study used satellite imagery taken in March, the peak of the hot, dry season. LST is recognised as a crucial element in fuel dehydration; nevertheless, in arid regions, other parameters such as NDDI and NBR are more critical in evaluating the risk of fire. This perspective is corroborated by Liu & Zhang (2015), who conducted a study during the extended dry season and found that the maximum temperature had the lowest coefficient value (0.064), while wind speed was the most significant factor, with a coefficient value of 12.21. Furthermore, the forest fire risk prediction map (FFRPM) equation developed by Nguyen & Tong (2023) indicated that NDDI had the highest weighting value of 0.30, whereas LST had a value of 0.15. Therefore, during the hot, dry season, factors other than temperature should be considered when predicting the likelihood of fire.

The distribution of wildfire occurrence was delineated and illustrated in Figure 4. The hazard zone map was determined to align with the elevated number of cases documented in March 2024. The findings indicate that the main towns of Kangar and Padang Besar are classified as "Very High Hazard" zones, with 29 and 15 occurrences, respectively. The main town was predominantly developed; nevertheless, interspersed among the

concrete were secondary forests, bushes, and shrubs. The current study suggests that human interference and excess heat from constructed environments may have affected fire incidence in those regions. The developed regions and high population density are widely recognised as factors contributing to elevated LST in the area, attributable to increased carbon emissions. This aligns with the findings of Zahran, Shams, and Said (2020), indicating a heightened risk of fire in densely populated areas. Similar findings were also confirmed by Moisa et al. (2023), who reported that the LST increased from 19 to 21°C in industrialised regions, indicating that the release of carbon stocks has led to temperature rises in their study area. Concurrently, the "Very Low Hazard" zone was predominantly located in the wooded regions of the Nakawan Range. This observation may be ascribed to the higher canopy density in wooded regions and their significant water-retention capacity, which delays evaporation and reduces LST readings. This perspective is supported by Rendana (2023), who asserts that the low fire risk classification was found in medium- to dense-forested areas. In addition, Nguyen & Tong (2023) indicated that the area with the least fire risk primarily comprises forests and mountains. These results provide the local authority with valuable information to plan conflagration mitigation measures, particularly during periods of extreme heat and drought.

CONCLUSION

The integration of multispectral indices with Geospatial analysis is a substantial enhancement in the ability to predict and mitigate wildfire-related dangers. This study successfully developed a Fire Hazard Index (FHI) by combining LST, NDVI, NDMI, NDWI, NDDI, and NBR data. The FHI effectively identifies the wildfire hazard zone within Perlis state by analysing the environmental and meteorological factors that contribute to wildfire occurrence. The results indicate that the "Very High Hazard" zone was primarily located in the developed areas, particularly in grasslands adjacent to the residences. The limited water retention capacity and the physical attributes of shrubs render them more susceptible to ignition by fire. The findings underscore the areas requiring increased focus from the local authorities, particularly the Fire and Rescue Department. The Fire Hazard Index is an essential tool for decision-making as climate change extends dry periods. It safeguards both natural ecosystems and human habitats from the catastrophic effects of uncontrolled wildfires.

REFERENCE

1. Anwarzaini, A. Z., & Tarmizi, N. M.(2025). Spatiotemporal Analysis of Wildfire Occurrence in Perlis from Year 2014 To 2024. Journal of Tourism Hospitality and Environment Management, 10(42),21–38. https://doi.org/10.35631/ JTHEM.1042003
2. Anucharan, T., Sroprom, T., Chaikaew, N., & Iamchuen, N. (2025). Assessing Burn Severity and Vegetation Impact Using Sentinel-2 Satellite Imagery and Geospatial Analysis in Mae Ka Subdistrict, Mueang District, Phayao, Thailand. Int. J. Geoinformatics, 21(4), 51–70.
3. Bandara, S., Navaratnam, S., & Rajeev, P. (2023). Bushfire Management Strategies: Current Practice, Technological Advancement and Challenges, Fire, 6(11). https://doi.org/10.3390/fire6110421.
4. Burapapol, K. & Nagasawa, R. (2016). Mapping Soil Moisture as an Indicator of Wildfire Risk Using Landsat 8 Images in Sri Lanna National Park, Northern Thailand, J. Agric. Sci., 8(10), 107. https://doi.org/10.5539/jas.v8n10p107.
5. Chew, Y. J., Ooi, S. Y., Pang, Y. H., and Wong, K. S. (2022). Trend Analysis of Forest Fire in Pahang, Malaysia from 2001-2021 with Google Earth Engine Platform, J. Logist. Informatics Serv. Sci., 9(4), 15–26. https://doi.org/10.33168/LISS.2022.0402.
6. Chew, Y. J., Ooi, S. Y., Pang, Y. H., and Lim, Z. Y. (2023). Investigating the Relationship between the Influencing Fire Factors and Forest Fire Occurrence in the Districts of Rompin, Pekan, and Kuantan in the State of Pahang, Malaysia, Using Google Earth Engine, Int. J. Adv. Sci. Eng. Inf. Technol., 13(5), 1733–1741. https://doi.org/10.18517/ijaseit.13.5.19026.
7. Fisal, N. S. M., Lintangah, W., and Ismenyah, M. (2017). Community Awareness & Challenges in Forest Fire Prevention: a Case Study At Peat Swamp Forest, Klias Forest Reserve, Beaufort, Sabah, Malaysia., Int. J. Agric. For. Plant., 5, 86–91.
8. Jamaruppin, M. E., Bayuaji, L., Ab Ghani, N., Rahman, M. A., Akashah, F. W., & Shah, A. (2016). Forest Fire Occurrence Analysis Based on Land Brightness Temperature using Landsat Data (Study Area: Jalan Kuantan–Pekan, Pahang, Malaysia), Natl. Conf. Postgrad. Res., 798–805.

9. Liu, D. & Zhang, Y. (2015). Research of regional forest fire prediction method based on multivariate linear regression, Int. J. Smart Home, 9(1), 13–22, https://doi.org/10.14257/ijsh.2015.9.1.02.
10. Mat Deli, M. (2023). Forest Fire Incident Forecasting System In Permanent Reserved Forest In Peninsular Malaysia Using Big Data Analytics, Sustain. Energy Environ. Rev., 1(1), 1–13. https://doi.org/10.59762/seer92471204112023110314 3053.
11. Moisa, M. B. et al. (2023). Analysing the correlation of forest and wetland with land surface temperature by using geospatial technology: a case of Yayo district, Southwestern Ethiopia, Geocarto Int., 38(1), https://doi.org/10.1080/10106049.2023.2256300.
12. Nguyen, T. T. N. & Tong, T. H. (2023). Wildfire Risks In The Southwest Of Ky Son District, Nghe An Province – A Multi-Critical Model, J. Sci. Tech., 7–18, https://doi.org/10.56651/lqdtu.jst.v6.n01.662.sce.
13. Rendana, M. et al. (2023). Current and future land fire risk mapping in the southern region of Sumatra, Indonesia, using CMIP6 data and GIS analysis, SN Appl. Sci., 5(8). https://doi.org/10.1007/s42452-023-05432-6.
14. Tarmizi, N. M., & Rizwan, N. I. (2024). Integrated Supervised Classification of LULC in Identifying Musang King Durian Illegal Farming Location. Jurnal Sylva Lestari, 12(2), 459–479. https://doi.org/10.23960/jsl.v12i2.856
15. Tarmizi, N. B. M., Anwarzaini, A. Z. B., & Fisol, M. F. B. M. (2025, August). Maximum Likelihood Classifier Analysis of UAV Image Classification Post-Fire Area Estimation. In 2025 IEEE 16th Control and System Graduate Research Colloquium (ICSGRC)(pp. 222–227). IEEE.
16. Thangavel, K. et al. (2023). Autonomous Satellite Wildfire Detection Using Hyperspectral Imagery and Neural Networks: A Case Study on Australian Wildfire, Remote Sens., 15 (3). https://doi.org/10.3390/rs15030720.
17. Zahran, E. S. M. M., Shams, S., & Said, S. N. M. B. M. (2020). Validation of forest fire hotspot analysis in GIS using forest fire contributory factors, Syst. Rev. Pharm., 11(12), 249–255. https://doi.org/10.31838/srp.2020.12.40.